

**Université Pierre et Marie Curie**  
**Master Sciences et Technologie (M2)**  
**Spécialité : Concepts fondamentaux de la physique**  
**Parcours : Physique des Liquides et Matière Molle**  
**Cours : Dynamique Non-Linéaire**

**Laurette TUCKERMAN**  
**laurette@pmmh.espci.fr**

**Practical Bifurcation Techniques and Nonlinear Tourism**  
**English-language version**

# Practical Bifurcation Techniques

## 1 Making the most of your data

We have studied many model equations and normal forms. But what can be done when we only have results from experiments, or from numerical simulations?

### 1.1 Locating the bifurcation threshold

The fastest and most precise way to locate a bifurcation threshold is to use growth or decay rates, not final states. There is a very fundamental reason for this. At a bifurcation, two things take place:

- new branches form, or existing branches intersect
- the critical eigenvalue goes through zero.

Because of the second property, it necessarily takes a long time to converge to a steady state near a bifurcation – theoretically an infinite time just at the bifurcation. This is called *critical slowing down*. However, a growth or decay rate can be measured long before convergence; see figure 1. The growth or decay rate is the slope of timeseries plotted on a logarithmic scale. Generally, the decay or growth rate varies linearly with the control parameter, e.g.  $\mu$ ,  $\text{Re}$ , or  $\text{Ra}$  near a bifurcation, for the simple reason that most functions are locally linear. Interpolation or extrapolation from just two values gives a very accurate estimate of the threshold; see figure 2. It is not necessary to calculate both positive values (growth) and negative values (decay); two values of either kind usually suffice.

#### Explanation and generalizations

–Although a multidimensional dynamical system has as many eigenvalues as it has dimensions, the evolution is quickly dominated by that with largest real part, i.e that associated with the slowest decay or with the fastest growth. Figure 1 shows the evolution of

$$x(t) = a_1 e^{\lambda_1 t} + a_2 e^{\lambda_2 t} + a_3 e^{\lambda_3 t} \quad (1)$$

with  $\lambda_1 = -1, -0.5, 0.5, 1, \lambda_2 = -4, \lambda_3 = -9, a_1 = 0.4, a_2 = 2, a_3 = 5$ . After an initial transient, the faster decay associated with  $\lambda_2, \lambda_3$  means that the timeseries resembles

$$x(t) \approx a_1 e^{\lambda_1 t} \quad (2)$$

This behavior leads to the *power method* for calculating eigenvalues. But there is no sure method to know when the asymptotic regime has been reached.

–Almost *any* quantity suffices to measure growth or decay rates (e.g. the temperature or velocity at one location). This is because almost all quantities have a non-zero projection onto the critical eigenmode.

–This procedure can be extended to localize Hopf bifurcation thresholds from oscillatory timeseries by plotting successive maxima, as shown in figure 3.

#### Some cautionary points

–The growth or decay rate is *from or to a steady state*  $\bar{x}$ ; i.e.  $(x(t) - \bar{x}) \sim e^{\lambda_1 t}$ . Thus, it is necessary to know the steady state  $\bar{x}$  as well as the timeseries  $x(t)$ . Sometimes one knows  $\bar{x}$  exactly. For a symmetry-breaking bifurcation,  $x$  can be chosen to measure the departure from symmetry, so that  $\bar{x} = 0$ .

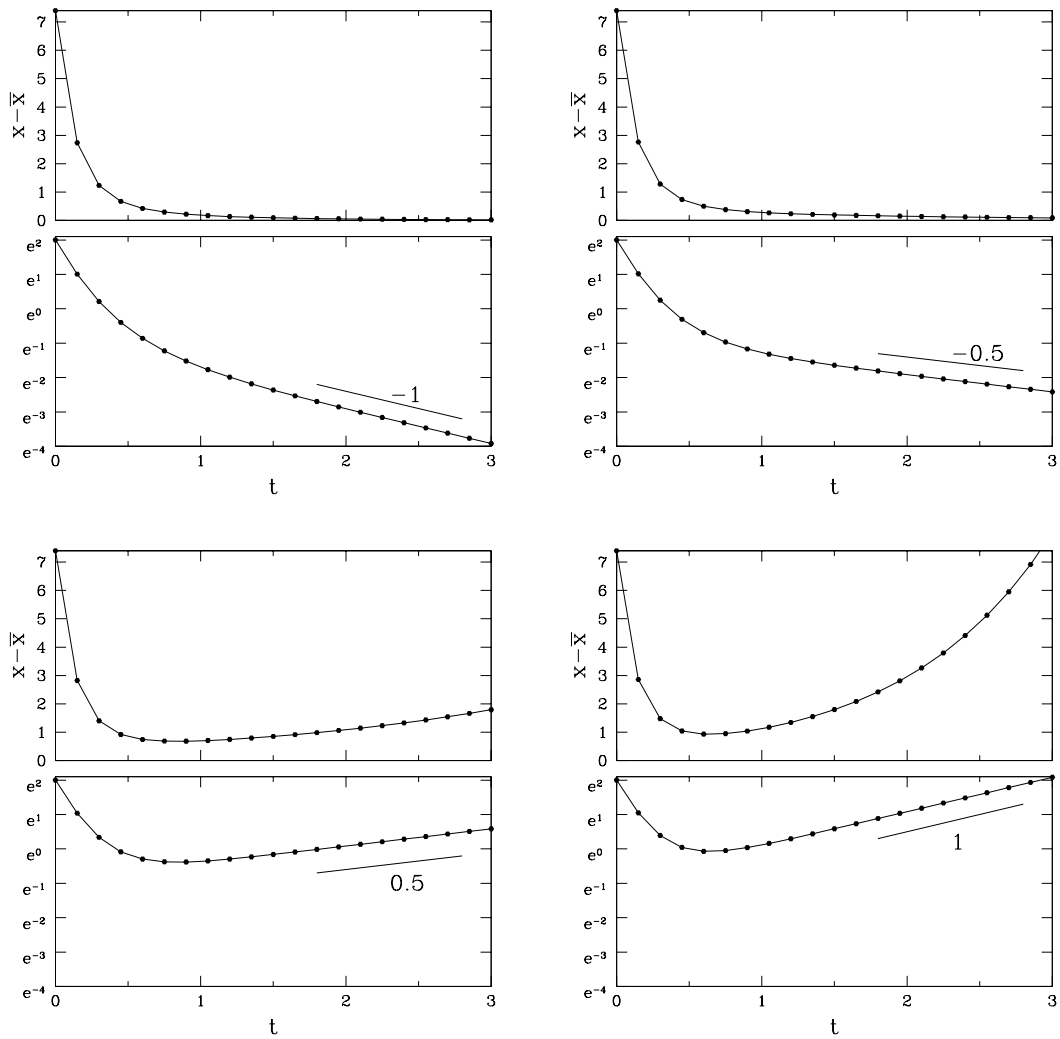


Figure 1: Determining the growth or decay rate from the latter part of a timeseries.

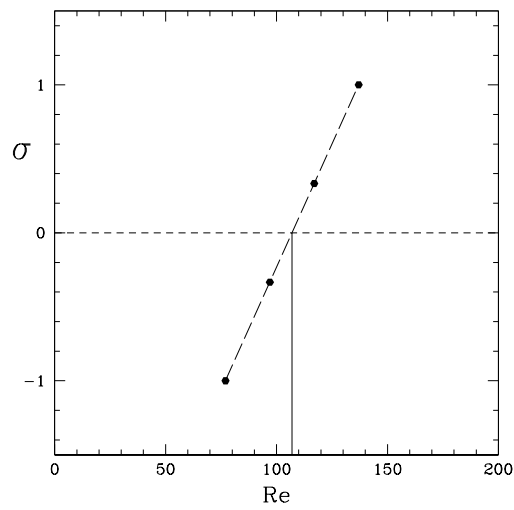


Figure 2: Determining the threshold by extrapolating or interpolating the growth or decay rates.

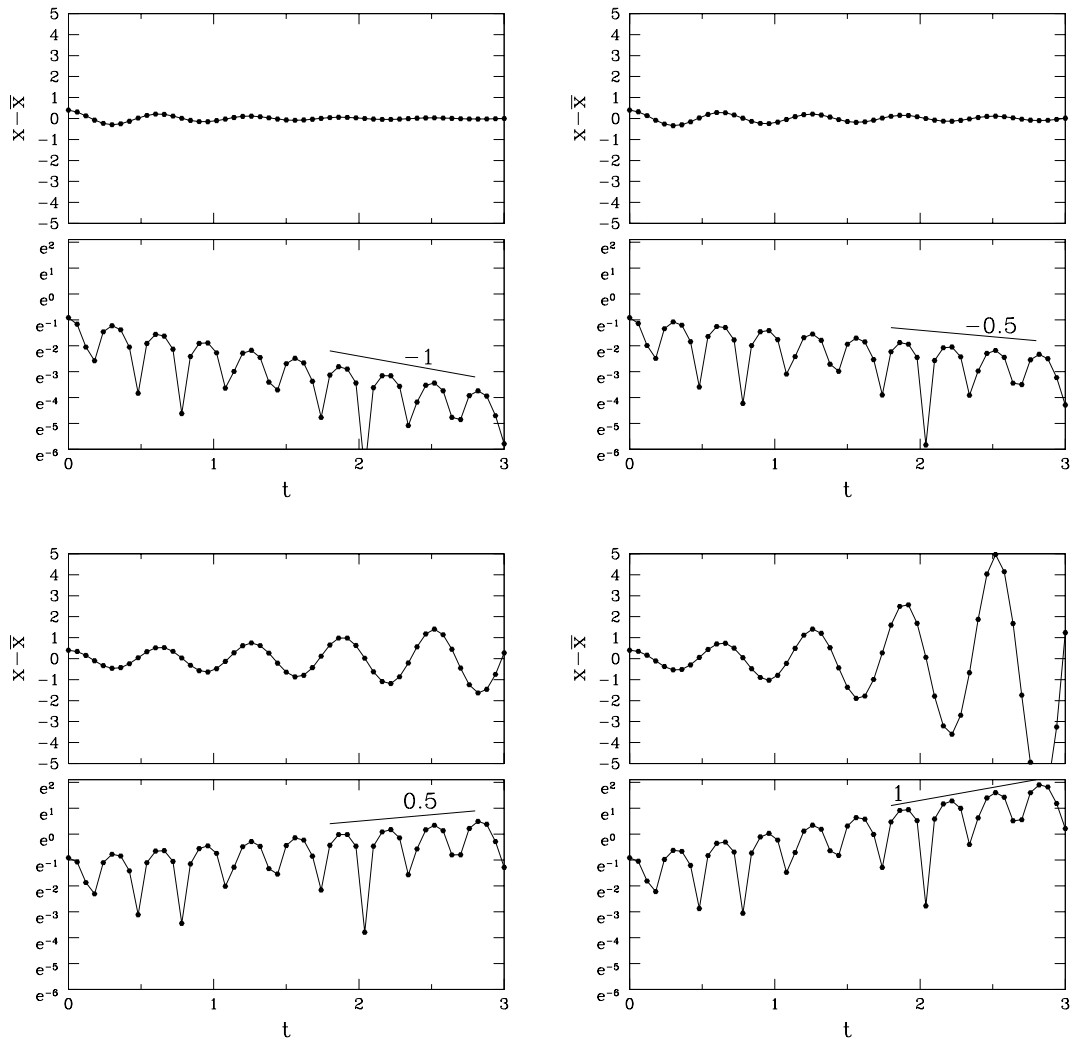


Figure 3: Determining the growth or decay rate from an oscillatory timeseries.

Numerically, another means such as Newton's method (see below) can be used to calculate the steady state. Otherwise, one can wait for (approximate) convergence to determine  $\bar{x}$ .

–The growth or decay rate varies linearly with the control parameter for many bifurcations, e.g. pitchfork, Hopf and transcritical bifurcations. An important exception is the saddle-node bifurcation, for which growth or decay rates vary like the square root of the distance from the threshold;

$$\begin{aligned} \frac{dx}{dt} = f(x) = \mu - x^2 &\implies \bar{x} = \pm\sqrt{\mu} \\ f'(x) = -2x &\implies f'(\bar{x}) = \mp 2\sqrt{\mu} \end{aligned}$$

Thus, near a suspected saddle-node bifurcation, the square of the growth or decay rate should be plotted as a function of the control parameter in order to locate the threshold.

## 1.2 Determining whether a bifurcation is supercritical or subcritical

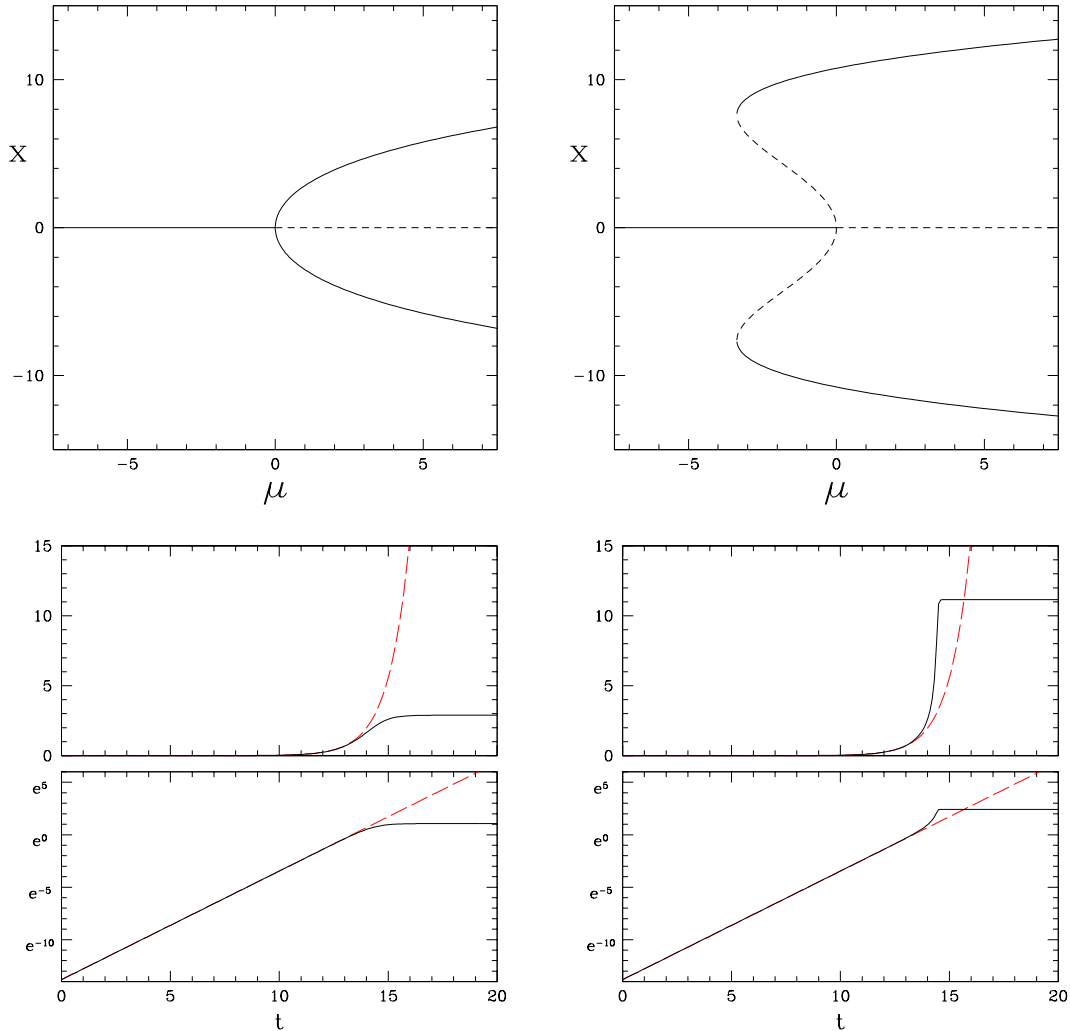


Figure 4: Determining whether a bifurcation is supercritical or subcritical from a timeseries just above the bifurcation point.

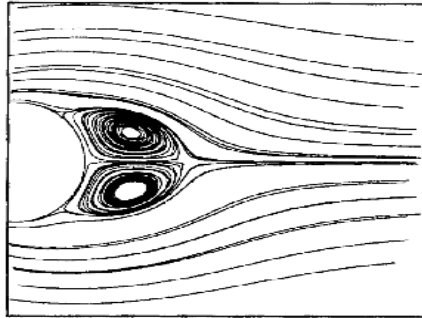
The most visible feature of a subcritical bifurcation is hysteresis: coexistence of two different steady states. However, as stated above, convergence to a steady state is slow near a bifurcation. Barkley's method (R.D. Henderson & D. Barkley, *Phys. Fluids* **8** 1783 (1996)), illustrated in figure 4, calls for examining a timeseries just above the bifurcation point to see if the initial deviation from exponential growth is positive or negative.

$$\dot{x} = \mu x + \alpha x^3 + \beta x^5 \quad (3)$$

For the panels on the left,  $\alpha = -0.116$  (supercritical bifurcation), while for those on right,  $\alpha = 0.116$  (subcritical bifurcation). For both cases  $\mu = 1.041$  and  $\beta = -0.001$ . The initial growth, while term  $\mu x$  dominates, is exponential (linear in the log scale below). Eventually the term  $\alpha x^3$  contributes, which causes the growth to slow down and saturate (left, supercritical case) or to speed up (right, subcritical case). In the subcritical case (right), it is the contribution  $\beta x^5$  that halts the growth and leads to saturation.

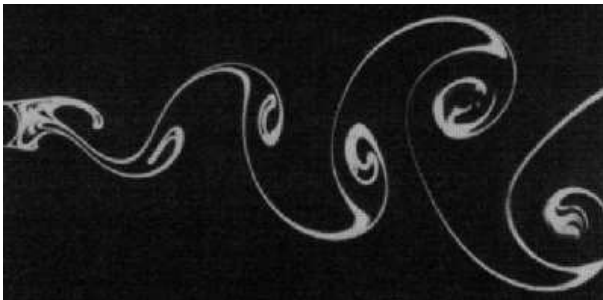
### 1.3 Freezing a symmetry

A complete understanding of a bifurcation scenario often requires the knowledge of unstable states. In the case of a symmetry-breaking bifurcation, this is easy and in fact, often happens inadvertently in numerical calculations. This is the case, for example, for the flow in the wake of a circular cylinder, illustrated in figure 5. Defining the coordinate system such that the imposed flow is in the  $x$  direction and the cylinder axis is in the  $z$  direction, the sequence of flows and transitions is as follows:



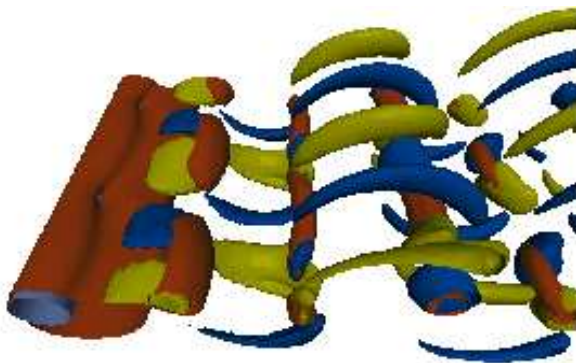
steady flow  
 $\left\{ \begin{array}{l} \text{reflection symmetry in } y \\ \text{homogeneous in } z \end{array} \right\}$

Hopf bifurcation  $\Downarrow$   $Re = 46$



periodic von Kármán  
 vortex street  
 $\left\{ \begin{array}{l} \text{spatio-temporal symmetry in } y \\ \text{homogeneous in } z \end{array} \right\}$

circle pitchfork  
 of limit cycle  $\Downarrow$   $Re = 188.5$



3D flow  
 $\left\{ \begin{array}{l} \text{spatio-temporal reflection symmetry in } y \\ \text{spatially periodic in } z \end{array} \right\}$

Figure 5: Flows and transitions for the wake of a circular cylinder.

Thus, if reflection symmetry is maintained, the transition to the von Kármán vortex street is suppressed. If a 2D calculation is carried out, then there is no transition to the 3D flow. In some cases, experimental versions of these symmetry-freezing tricks can also be implemented.

## 2 Numerical techniques

The sections which follow concern only numerical calculation and not experiments.

### 2.1 Timestepping and stability of schemes

Digital computers cannot actually carry out continuous operations. Any numerical method for time integration is actually a transformation of the differential equation into a discrete-type dynamical system. (For now, we do not address spatial discretization, the approximation of functions of space by a finite number of values.)

Let us examine some of the simplest methods for solving

$$\frac{du}{dt} = f(u) \quad (4)$$

The forward Euler method is just the first-order Taylor expansion:

$$u(t + \Delta t) = u(t) + f(u(t))\Delta t \quad (5)$$

This is called an *explicit* method because  $f$  is evaluated at the previous time step. The backward Euler method is:

$$u(t + \Delta t) = u(t) + f(u(t + \Delta t))\Delta t \quad (6)$$

This is called an *implicit* method, since the above equation must be solved for  $u(t + \Delta t)$  by a not-necessarily-trivial procedure. Note that this method also matches the Taylor expansion to first order, since

$$f(u(t + \Delta t)) = f(u(t) + u'(t)\Delta t) = f(u(t)) + f'(u(t))u'(t)\Delta t + \dots \quad (7)$$

Both methods are called first-order accurate.

Analysis is usually done on linear equations, such as

$$\frac{du}{dt} = -qu \quad (8)$$

for which everything is understood analytically and a single exact timestep would be:

$$u(t + \Delta t) = e^{-q\Delta t}u(t) \quad (9)$$

On this equation, the forward Euler method leads to

$$u(t + \Delta t) = u(t) - qu(t)\Delta t = (1 - q\Delta t)u(t) \quad (10)$$

while the backward Euler method leads to

$$u(t + \Delta t) = u(t) - qu(t + \Delta t)\Delta t \quad (11a)$$

$$(1 + q\Delta t)u(t + \Delta t) = u(t) \quad (11b)$$

$$u(t + \Delta t) = \frac{1}{1 + q\Delta t}u(t) \quad (11c)$$

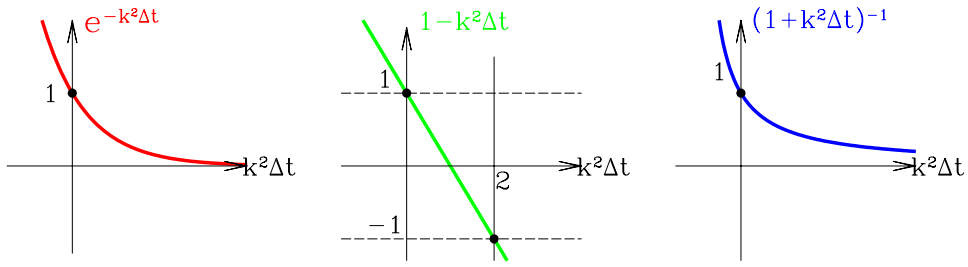


Figure 6: One-step amplification factors for the exact evolution, forward Euler, and backward Euler methods.

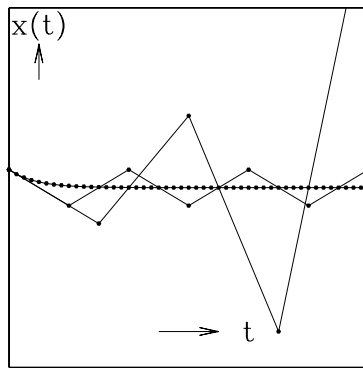


Figure 7: Integration of  $\dot{u} = -k^2 u$  using forward Euler method with  $k^2 \Delta t = 0.25$  (decay to zero), 2 (neutral oscillations), 3 (growing oscillations).

This analysis is valuable for understanding diffusive equations, where a Fourier representation of the solution  $u$  leads to:

$$\partial_t u = \partial_{xx}^2 u \quad (12)$$

$$u(x, t) = \sum_{k=1}^{k_{max}} u_k(t) \sin kx \quad (13)$$

$$\dot{u}_k = -k^2 u_k \quad (14)$$

The timestepping schemes replace the exponential multiplicative factor by the factors shown in figure 6.

We see that the forward Euler method leads to *growing oscillations* instead of decrease for  $k^2 \Delta t > 2$ , as shown in figure 7. That is, one is constrained to use the timestep  $\Delta t < 2/k_{max}^2$ . One says that this method is not absolutely stable (or A-stable). A method is said to be A-stable if, when used to solve  $\dot{u} = qu$  with  $Re(q) < 0$ , the numerical solution tends to zero.

We see that the forward Euler method leads to *growing oscillations* Let us illustrate from the dynamical-systems point of view the consequences of using the unstable forward Euler method on the standard dynamical system

$$\dot{x} = \mu x - x^3 \quad (15)$$

This is the standard normal form for a supercritical pitchfork bifurcation, with solution  $x = 0$  (stable for  $\mu \leq 0$ , unstable for  $\mu > 0$  and  $x = \pm\sqrt{\mu}$  for  $\mu > 0$ ).

The system (15) is to be integrated numerically in time using the timestepping scheme

$$x(t + \Delta t) = x(t) + \Delta t(\mu x(t) - x(t)^3)$$

for timestep  $\Delta t > 0$ , leading to the discrete-time dynamical system

$$x_{n+1} = f(x_n) \equiv x_n + \Delta t(\mu x_n - x_n^3) \quad (16)$$

where  $x_n = x(n\Delta t)$ .

The steady states are solutions to

$$\bar{x} = \bar{x} + \Delta t(\mu \bar{x} - \bar{x}^3)$$

and hence the same as for the continuous-time system, i.e.  $\bar{x} = 0$  and  $\bar{x} = \pm\sqrt{\mu}$  for  $\mu > 0$ .

Their stability is determined by calculating

$$\begin{array}{ll} f'(x) = 1 + \Delta t(\mu - 3x^2) & \\ f'(0) = 1 + \Delta t\mu & f'(\pm\sqrt{\mu}) = 1 + \Delta t(\mu - 3\mu) = 1 - 2\Delta t\mu \\ -1 < 1 + \Delta t\mu < 1 & -1 < 1 + \Delta t(\mu - 3\mu) = 1 - 2\Delta t\mu < 1 \\ -2 < \Delta t\mu < 0 & -2 < -2\Delta t\mu < 0 \\ -2/\Delta t < \mu < 0 & 0 < \mu < 1/\Delta t \end{array}$$

(Recall that the timestep  $\Delta t$  is necessarily positive.)

Thus, there is a steady bifurcation at  $\mu = 0$ , clearly a pitchfork bifurcation, since the two new branches of steady states are created there, just as in the continuous system. But there are also period doubling bifurcations at  $\mu = -2/\Delta t$ , where  $f'(0) = -1$ , and at  $\mu = 1/\Delta t$ , where  $f'(\pm\sqrt{\mu}) = -1$ .

The super or subcriticality of these period-doubling bifurcations can be ascertained as follows.

$$x_{n+1} = x_n(1 + \Delta t(\mu - x_n^2))$$

We set  $\mu = -2/\Delta t + \delta$ . Perturbations to  $x = 0$  grow in an oscillatory manner when the multiplicative factor satisfies

$$\begin{array}{l} 1 + \Delta t \left( \frac{-2}{\Delta t} + \delta - x_n^2 \right) < -1 \\ 1 + (-2 + \delta\Delta t - x_n^2\Delta t) < -1 \\ -1 + (\delta\Delta t - x_n^2\Delta t) < -1 \\ \delta\Delta t - x_n^2\Delta t < 0 \\ \delta < x_n^2 \end{array}$$

Thus, all perturbations to  $x = 0$  grow when  $\delta < 0$  (i.e. for  $\mu < -2/\Delta t$ ), and sufficiently large perturbations to  $x = 0$  grow for  $\delta > 0$  (i.e. for  $\mu > -2/\Delta t$ ). This implies that the two-cycle exists for  $\delta > 0$ , where  $x = 0$  is stable, and hence that the period doubling bifurcation at  $\mu = -2/\Delta t$  is subcritical.

(Demonstrating the subcriticality of the period-doubling bifurcations at  $\mu = 1/\Delta t$ ,  $x = \pm\sqrt{\mu}$  is more difficult.)

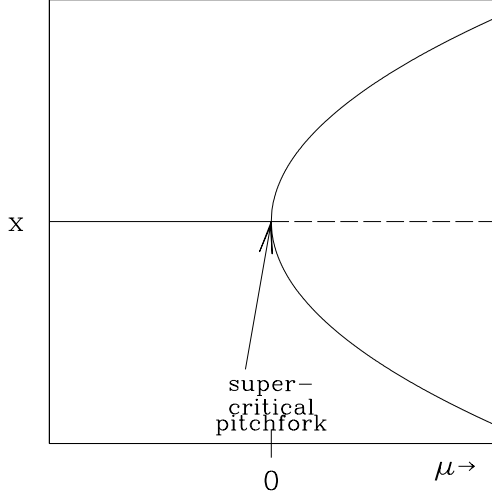


Figure 8: Time-continuous system.

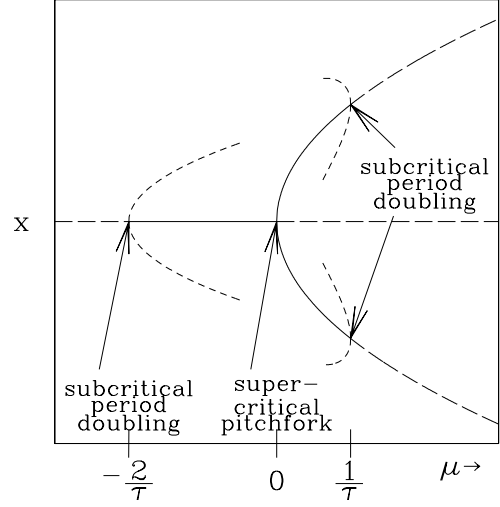


Figure 9: Time-discretized system.

Similar analyses can be carried out on methods which are of higher order in time, i.e. which match the Taylor series to higher order. the explicit 2nd-order *Adams-Bashforth method* uses two previous timesteps to construct the next guess:

$$u(t + \Delta t) = u(t) + \frac{\Delta t}{2} (3f(u(t)) - f(u(t - \Delta t))) \quad (17)$$

It can be verified to be second-order accurate by expanding as a Taylor series of  $u(t)$ .

Stability analysis of the Adams-Bashforth method is more complicated, since it relies on two previous steps. We write the method applied to  $\dot{u} = -k^2 u$  as follows:

$$\begin{pmatrix} u(t + \Delta t) \\ u(t) \end{pmatrix} = \begin{pmatrix} u(t) - \frac{k^2 \Delta t}{2} (3u(t) - u(t - \Delta t)) \\ u(t) \end{pmatrix} = \begin{pmatrix} 1 - \frac{3k^2 \Delta t}{2} & \frac{k^2 \Delta t}{2} \\ 1 & 0 \end{pmatrix} \begin{pmatrix} u(t) \\ u(t - \Delta t) \end{pmatrix} \quad (18)$$

The eigenvalues of a matrix  $\begin{pmatrix} a & b \\ c & 0 \end{pmatrix}$  are

$$\lambda = \frac{a}{2} \pm \sqrt{\left(\frac{a}{2}\right)^2 + bc} \quad (19)$$

We seek values values of  $k^2 \Delta t$  such that the Adams-Bashforth method is stable, i.e.  $|\lambda| \leq 1$ .

$$\pm 1 = \frac{a}{2} \pm \sqrt{\left(\frac{a}{2}\right)^2 + bc} \quad (20)$$

$$\pm 1 - \frac{a}{2} = \pm \sqrt{\left(\frac{a}{2}\right)^2 + bc} \quad (21)$$

$$\left(\pm 1 - \frac{a}{2}\right)^2 = \left(\frac{a}{2}\right)^2 + bc \quad (22)$$

$$1 \mp a = bc \quad (23)$$

$$1 \mp \left(1 - \frac{3k^2 \Delta t}{2}\right) = \frac{k^2 \Delta t}{2} \quad (24)$$

$$0 = -k^2 \Delta t \quad \text{or} \quad 2 = k^2 \Delta t \quad (25)$$

The endpoints of the stability interval are  $0 \leq \Delta t \leq 2/k^2$ , just as they are for the forward Euler method.

In fact, no explicit method can be A-stable. This is because all explicit methods essentially approximate the exponential function  $\exp(q\Delta t)$  by a polynomial  $\sum_n c_n(q\Delta t)^n$ . For  $\text{Re}(q) < 0$ ,  $\exp(q\Delta t) < 1$ , while  $|\sum_n c_n(q\Delta t)^n| > 1$  for  $\Delta t$  sufficiently large. The explicit methods we have seen above are the 1st-order forwards Euler and 2nd-order Adams-Bashforth methods; the popular Runge-Kutta methods are also explicit methods. The only methods that can be A-stable are implicit and at most second-order.

The implicit *Crank-Nicolson or trapezoidal method* is an average of the forward and backward Euler formulas:

$$u(t + \Delta t) = u(t) + \frac{\Delta t}{2}(f(u(t)) + f(u(t + \Delta t))) \quad (26)$$

In terms of stability, using the test equation  $\dot{u} = -k^2 u$ , the Crank-Nicolson method yields

$$u(t + \Delta t) = \frac{1 - k^2 \Delta t / 2}{1 + k^2 \Delta t / 2} u(t) \quad (27)$$

For  $\Delta t > 0$ , this factor is always between  $-1$  and  $1$ , but as  $k \rightarrow \infty$ , it approaches  $-1$  as illustrated in figure 2.1, meaning that the amplitudes of Fourier components with high spatial frequencies oscillate in time, rather than being damped as they should be.

The implicit *backward differentiation method*

$$\frac{3}{2}u_{n+1} - 2u_n + \frac{1}{2}u_{n-1} = \Delta t f(u_{n+1}) \quad (28)$$

is second order and also has the desirable property that its amplification factor goes to 0 as  $\Delta t \rightarrow \infty$  for  $\text{Re}(q) < 0$ , as shown in figure 2.1.

Essentially, implicit methods can be A-stable because they approximate  $\exp(q\Delta t)$  by a rational function  $\sum_n c_n(q\Delta t)^n / \sum_m d_m(q\Delta t)^m$  and rational functions can be bounded for all values of  $\Delta t$ , as we have seen for the 1st-order backward Euler and 2nd-order Crank-Nicolson methods. Evaluating a rational function is, of course, hardly more difficult than evaluating a polynomial: the difficulty of implicit methods lies in applying them to other than the simple test problem  $\dot{u} = qu$ . In just one dimension, recalling that the backward Euler method is:

$$u(t + \Delta t) = u(t) + \Delta t f(u(t + \Delta t)) \quad (29)$$

the above occasion must usually be solved if  $f(u)$  is a nonlinear function. Far more frequently,  $u$  and  $f$  are multidimensional. In particular, if the equation to be solved is a PDE (partial differential equation), then the number of unknowns is the number of gridpoints times the number of variables. For example, for a single variable on a modest grid of size  $50 \times 50 \times 50$ , the number of unknowns is 125 000. For three velocity components on a  $100 \times 100 \times 100$  grid, the number of unknowns is  $3 \times 10^6$ . In this case, even if  $f$  is linear, i.e. a matrix operator, a large linear system must be inverted:

$$u(t + \Delta t) = u(t) + \Delta t M(u(t + \Delta t)) \implies \quad (30)$$

$$(I - \Delta t M)^{-1} u(t + \Delta t) = u(t) \quad (31)$$

Large linear systems will be discussed in the next section.

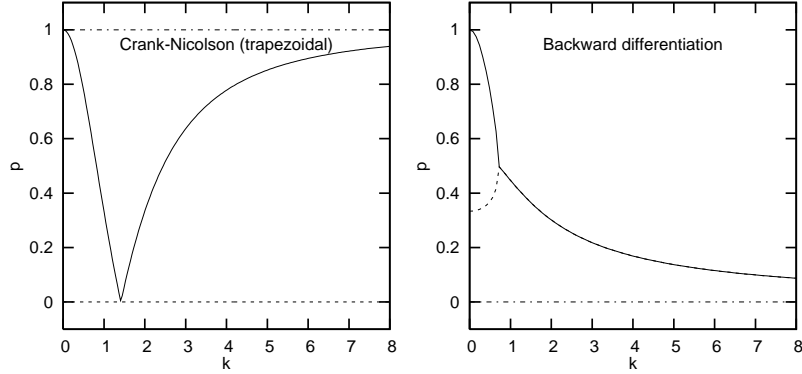


Figure 10: The amplification factor or factors for A-stable one- and two-step schemes.

## 2.2 Newton's method

Another method of calculating unstable steady states in Newton's method. In fact, Newton's method is useful even when the steady states sought are stable, because it is much faster than integrating in time.

Newton's method is based on the fact that functions are usually locally linear. Thus if we seek the root  $\bar{x}$  of  $f(x)$ , we can approximate it by the root of the local linear approximation to  $f(x)$ :

$$0 = f(\bar{x}) \approx f(x^{(0)}) + f'(x^{(0)})(\bar{x} - x^{(0)}) \implies \bar{x} \approx x^{(0)} - \frac{f(x^{(0)})}{f'(x^{(0)})} \quad (32)$$

Of course, since (32) is only an approximation, the value obtained for  $\bar{x}$  will not be accurate. We iterate the process as follows:

$$f'(x^{(n)})\Delta x = f(x^{(n)}) \quad (33a)$$

$$x^{(n+1)} = x^{(n)} - \Delta x \quad (33b)$$

Figure 11 illustrates this procedure. Figure 11 also shows that convergence of Newton's method is independent of the sign of  $f'$ , i.e. of the stability of the fixed point  $\bar{x}$ .

In the multidimensional case,  $f$  and  $x$  are vectors and the derivative is replaced by the Jacobian:

$$[Df(x^{(n)})]\Delta x = f(x^{(n)}) \quad (34a)$$

$$x^{(n+1)} = x^{(n)} - \Delta x \quad (34b)$$

where the matrix of partial derivatives  $[Df]_{ij} = \partial f_i / \partial x_j$  is evaluated at  $x^{(n)}$ .

For large dynamical systems, it may be difficult to solve the linear system (34). There are two types of methods for solving linear systems:

**Direct:** Other names are Gaussian elimination, LU decomposition, forward and backward substitution. For a matrix  $A$ , it is possible to write:

$$A = LU \quad (35)$$

where  $L$  is lower triangular and  $U$  is upper triangular. If  $A$  is a general  $N \times N$  matrix, this step requires  $O(N^3)$  operations. Then one solves

$$Ax = b \iff LUx = b \iff Ly = b \iff Ux = y \quad (36)$$

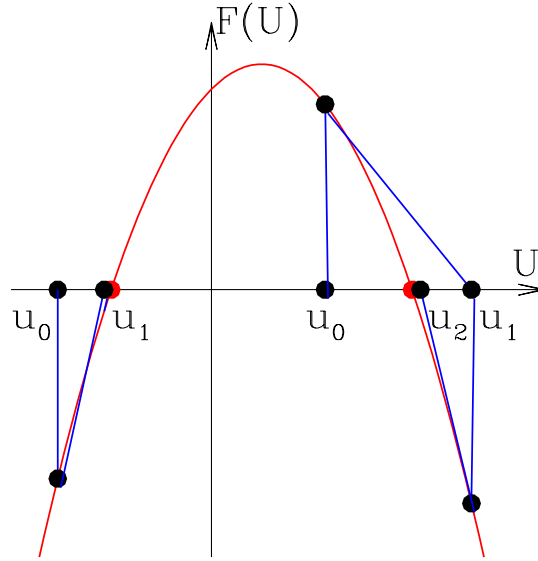


Figure 11: Newton's method finds a root  $\bar{x}$  of  $f$  by repeated linear extrapolation independent of the sign of  $f'$ .

This step requires  $O(N^2)$  operations for a general  $N \times N$  matrix. For a banded matrix with  $J$  bands, the LU decomposition requires  $O(J^2N)$  operations and the backsolve requires  $O(JN)$  operations. The rows and/or columns may need to be interchanged (called pivoting) if the elements are along the diagonal are much smaller than the off-diagonal elements.

**Iterative:** There are many sorts of iterative methods. Here we mention only methods of the family called conjugate gradient, or Krylov. By acting (multiplying) the right-hand-side  $b$  repeatedly by the matrix  $A$ , one generates a set of vectors (*Krylov* vectors), a linear combination of which is used to construct an approximation to the unknown vector  $x$ .

$$b \implies Ab \implies A^2b \implies \dots A^{K-1}b \quad (37a)$$

$$\text{Orthogonalize to form } v_1, v_2, \dots, v_K \quad (37b)$$

$$x \approx \sum_{k=1}^K c_k v_k \quad (37c)$$

The success of this method depends a great deal on the nature of the matrix  $A$ . If  $K = N$ , then (in exact arithmetic and for a non-singular matrix)  $N$  independent vectors are generated, from which it is necessarily possible to construct the solution. Since each matrix-vector product requires  $O(N^2)$  operations, generating  $N$  vectors requires  $O(N^3)$ , the same order as for direct methods. There are two ways in which iterative methods can save time:

–The matrix can be such that a matrix-vector product takes less than  $O(N^2)$  operations. This is the case if a matrix is sparse, for example, but even if it is not sparse, its entries can make this so. An example is the Fourier transform, which, as a linear process, is equivalent to multiplication by a matrix, but which takes  $O(N \log N)$  operations.

–A much smaller number  $K \ll N$  of the Krylov vectors may be needed to approximate the solution. This is the case if the matrix is *well-conditioned*, meaning essentially that the ratio of largest to smallest

eigenvalue is not too large, so that the matrix is not too far from the identity.

Iterative methods save space as well as time. The LU decomposition of a general sparse matrix  $A$  is not sparse – only bandedness is preserved. Thus the LU decomposition will generally require  $O(N^2)$  storage, even if  $A$  is sparse. In contrast, if only matrix-vector multiplies are required, the sparsity of  $A$  is preserved. In addition, iterative methods may use a procedure for carrying out the matrix-vector multiplications which does not require storage of the matrix  $A$  at all.

When Newton’s method is used to find the complex roots of  $z^3 - 1$ , it can converge to any of the three roots, depending on the initial condition. The set of initial conditions converging to each of the three roots forms a well-known fractal called a Julia set.

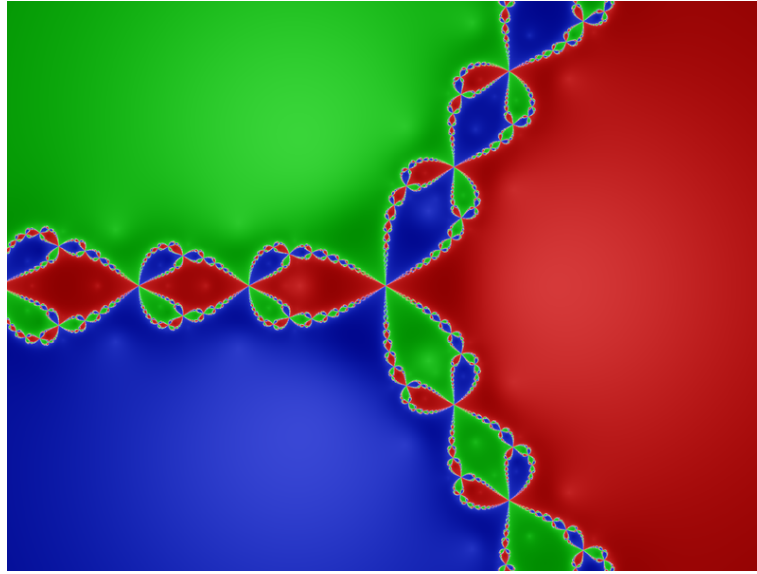


Figure 12: Basins of attraction for Newton’s method to the three roots of  $z^3 - 1$ .

### 2.3 Linearizing a code

Newton’s method (34) requires the Jacobian  $DF$ . As stated above, iterative methods can use a procedure which calculates the matrix-vector product instead of explicitly constructing the Jacobian matrix. This is often easier conceptually as well. For example, the Navier-Stokes equations

$$\partial_t \mathbf{U} = -(\mathbf{U} \cdot \nabla) \mathbf{U} - \nabla P + \frac{1}{\text{Re}} \Delta \mathbf{U} \quad (38)$$

$$\nabla \cdot \mathbf{U} = 0 \quad (39)$$

are linearized as follows:

$$\partial_t \mathbf{u} = -(\mathbf{U} \cdot \nabla) \mathbf{u} - (\mathbf{u} \cdot \nabla) \mathbf{U} - \nabla p + \frac{1}{\text{Re}} \Delta \mathbf{u} \quad (40)$$

$$\nabla \cdot \mathbf{u} = 0 \quad (41)$$

If we have a numerical method for solving the Navier-Stokes equations, we can easily transform it to a code for solving the linearized Navier-Stokes equations. This is analogous to the change

$$F(U) \implies DF(U)u \quad (42)$$

## 2.4 Power method

The simplest method for calculating eigenvalues and eigenvectors relies on the fact that repeated action of a matrix leads to growth and decay of the various eigenvectors according to their eigenvalues. Let the eigenvectors and eigenvalues of  $A$  be  $\mu_k, \phi_k$ :

$$A\phi_k = \mu_k\phi_k \quad (43)$$

with  $|\mu_1| > |\mu_2| > |\mu_3| > \dots$ . An arbitrary initial vector  $u^{(1)}$  will have components along each  $\phi_k$

$$u^{(1)} = \sum_k c_k \phi_k \quad (44)$$

Repeated multiplication by  $A$  generates

$$u^{(n)} = A^{n-1}u_1 = \sum_k c_k \mu_k^n \phi_k \rightarrow c_1 \mu_1^n \phi_1 \quad (45)$$

Thus  $u^{(n)}$  is parallel to the eigenvector  $\phi_1$  and an approximation to the *dominant eigenvalue*  $\mu_1$  (that of largest absolute value) is given by the Rayleigh quotient

$$\frac{\langle u^{(n+1)}, u^{(n)} \rangle}{\langle u^{(n)}, u^{(n)} \rangle} \approx \frac{c_1 \mu_1^{2n+1} \langle \phi_1, \phi_1 \rangle}{c_1 \mu_1^{2n} \langle \phi_1, \phi_1 \rangle} = \mu_1 \quad (46)$$

For finding the *leading eigenvalue* (that of largest real part), the exponential of the matrix can be used since

$$e^{A\Delta t} \phi_k = e^{\Delta t \mu_k} \phi_k \quad (47)$$

and leading eigenvalues are mapped into dominant ones by the exponential mapping.

## 3 Some mathematical techniques

Here we present some important mathematical constructions used in bifurcation problems.

### 3.1 Center manifold reduction

Consider a system undergoing a bifurcation whose Jacobian has mostly negative eigenvalues and one or more eigenvalues that are zero (for complex eigenvalues, we are referring to the real part). We diagonalize the Jacobian and use coordinates corresponding to the eigenvectors. We write the directions corresponding to the zero eigenvalues as the vector  $\mathbf{x}$  and those corresponding to the negative eigenvalues as vector  $\mathbf{y}$ .

$$\dot{\mathbf{x}} = A\mathbf{x} + f(\mathbf{x}, \mathbf{y}) \quad (48a)$$

$$\dot{\mathbf{y}} = B\mathbf{y} + g(\mathbf{x}, \mathbf{y}) \quad (48b)$$

where  $A$  and  $B$  are the Jacobian reduced to  $\mathbf{x}$  and  $\mathbf{y}$  respectively. We assume that the negative eigenvalues are bounded away from zero, and so  $\mathbf{y}$  evolves very quickly compared to  $\mathbf{x}$ . After a short initial transient, we say that  $\mathbf{y}$  is “slaved” to  $\mathbf{x}$  and write:

$$0 = B\mathbf{y} + g(\mathbf{x}, \mathbf{y}) \quad (49)$$

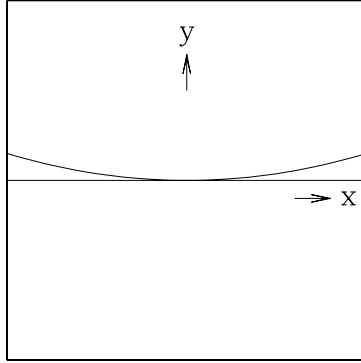


Figure 13: Center manifold reduction. The  $y$  dynamics can be considered to be passive, following the  $x$  dynamics.

relating  $y$  and  $x$  which implicitly gives  $y$  as a function of  $x$ , so that in principle:

$$\mathbf{y} = \mathbf{h}(\mathbf{x}) \quad \text{with } \mathbf{y} = O(|\mathbf{x}|^2) \quad (50)$$

In practice, (49) is solved approximately by expanding  $\mathbf{h}(\mathbf{x})$  as a series, whose elements are monomials in the components of  $\mathbf{x}$  and  $\mathbf{y}$ . We then substitute the exact or approximate  $\mathbf{h}(\mathbf{x})$  into (48a) to obtain:

$$\dot{\mathbf{x}} = A\mathbf{x} + f(\mathbf{x}, \mathbf{h}(\mathbf{x})) \quad (51a)$$

The **Reduction Principle** states that system (48) is locally topologically equivalent near the origin to (51a) with

$$\dot{\mathbf{y}} = B\mathbf{y} \quad (51b)$$

in which  $\mathbf{x}$  and  $\mathbf{y}$  are decoupled.

### 3.2 Fredholm alternative

The statement of the Fredholm alternative for self-adjoint operators is as follows. Suppose  $A$  is a singular linear operator and  $\zeta$  its null vector, i.e. such that

$$A\zeta = 0 \quad (52)$$

Then the equation

$$A\mathbf{x} = \mathbf{b} \quad (53)$$

has a solution if and only if

$$\langle \zeta, \mathbf{b} \rangle = 0 \quad (54)$$

The solution to (53), if it exists, is non-unique since any multiple of  $\zeta$  can be added to  $\mathbf{x}$ , and we may choose it to be orthogonal to the null vector:

$$\langle \zeta, \mathbf{x} \rangle = 0 \quad (55)$$

If  $A$  is not self adjoint, then its adjoint  $A^\dagger$  also has a null vector

$$A^\dagger \zeta^\dagger = 0 \quad (56)$$

and (54)-(55) are generalized to

$$\langle \zeta^\dagger, \mathbf{b} \rangle = 0 \quad (57)$$

$$\langle \zeta^\dagger, x \rangle = 0 \quad (58)$$

where  $\zeta^\dagger$  is the null eigenvector of the adjoint operator  $A^\dagger$  or, equivalently, the left eigenvector of  $A$ .

One direction is easy to show. Taking the inner product of (53) with the null vector  $\zeta^\dagger$  leads to:

$$\langle \zeta^\dagger, \mathbf{b} \rangle = \langle \zeta^\dagger, A\mathbf{x} \rangle = \langle A^\dagger \zeta^\dagger, \mathbf{x} \rangle = 0 \quad (59)$$

Thus, (53) implies (57). The other direction is more difficult to show in the abstract, but is also simple in finite dimensions. If  $A$  is a singular matrix and  $\zeta$  its null vector, then we can carry out a change of basis such that the new  $A$  has zeroes in its first row. Equation (57) then merely says that any vector of the form  $Ax$  must have zero as its first component. This is because the new  $A^\dagger$  has zeroes in its first column, the new  $\zeta^\dagger$  is the first unit vector, and the inner product of a vector with  $\zeta^\dagger$  is the first component. Thus, equation (53) becomes

$$A\mathbf{x} = \mathbf{b} \quad (60)$$

$$\begin{bmatrix} 0 & 0 & 0 & 0 \\ X & X & X & X \\ X & X & X & X \\ X & X & X & X \end{bmatrix} \begin{bmatrix} x \\ y \\ z \\ w \end{bmatrix} = \begin{bmatrix} a \\ b \\ c \\ d \end{bmatrix}$$

where  $X$  designates entries of  $A$  that are not necessarily zero. Equation (56) becomes

$$A^\dagger \zeta^\dagger = 0 \quad (61)$$

$$\begin{bmatrix} 0 & X & X & X \\ 0 & X & X & X \\ 0 & X & X & X \\ 0 & X & X & X \end{bmatrix} \begin{bmatrix} 1 \\ 0 \\ 0 \\ 0 \end{bmatrix} = \begin{bmatrix} 0 \\ 0 \\ 0 \\ 0 \end{bmatrix}$$

and equation (57) becomes

$$\langle \zeta^\dagger, \mathbf{b} \rangle = [1 \ 0 \ 0 \ 0] \begin{bmatrix} a \\ b \\ c \\ d \end{bmatrix} = a = 0 \quad (62)$$

The condition (62) suffices for (60) to have a solution if there are no remaining null vectors, since then the remaining lower  $3 \times 3$  matrix of  $A$  is non-singular. If there are other null vectors, then the right-hand-side  $\mathbf{b}$  must be orthogonal to these as well.

### 3.3 Constructing bifurcating solutions

We now illustrate how the Fredholm alternative is used to construct solution branches in the neighborhood of a bifurcation point. This treatment is taken from

G. Iooss, *Bifurcations successives et stabilité*, Journal de Physique, **39**, C5-99 (1978).

We begin with an evolution equation for a field  $u$  with a term  $\mathcal{L}$  which is linear in  $u$  and which depends on a control parameter  $r$ , and a term  $\mathcal{N}$  which is quadratic in  $u$ :

$$\partial_t u = \mathcal{L}(r)u + \mathcal{N}(u, u) \quad (63)$$

The trivial solution  $u = 0$  undergoes a steady bifurcation at  $r = 0$ . Thus  $\mathcal{L}_0 \equiv \mathcal{L}(r = 0)$  has a null vector  $\zeta$ :

$$0 = \mathcal{L}_0 \zeta \quad (64)$$

as well as an adjoint null vector  $\zeta^\dagger$

$$0 = \mathcal{L}_0^\dagger \zeta^\dagger \quad (65)$$

which we take to be normalized

$$\langle \zeta^\dagger, \zeta \rangle = 1 \quad (66)$$

Finally, we will assume that the bifurcating eigenvalue crosses zero transversely

$$\sigma(r = 0) = 0 \quad \sigma'(r = 0) \neq 0 \quad (67)$$

which leads (for reasons we will not explain here) to the condition:

$$\langle \zeta^\dagger, \mathcal{L}_1 \zeta \rangle \neq 0 \quad (68)$$

We are interested in the behavior of steady solutions near  $r = 0$ . We expand  $\mathcal{L}$  and  $\mathcal{N}$  in powers of  $r$ :

$$\mathcal{L}(r) = \mathcal{L}_0 + r\mathcal{L}_1 + r^2\mathcal{L}_2 + \dots \quad (69a)$$

$$\mathcal{N}(u, u) = \mathcal{N}_0(u, u) + r\mathcal{N}_1(u, u) + r^2\mathcal{N}_2(u, u) \quad (69b)$$

We then expand the solution  $u$  and control parameter  $r$  in powers of some small parameter  $\epsilon$ :

$$u = u_1\epsilon + u_2\epsilon^2 + \dots \quad (69c)$$

$$r = r_1\epsilon + r_2\epsilon^2 + \dots \quad (69d)$$

where  $u$  and  $r$  contain no  $O(1)$  terms because we are considering a solution bifurcating from  $u = 0$  at  $r = 0$ . Substituting the expansions (69) into (63) leads to:

$$\begin{aligned} 0 &= (\mathcal{L}_0 + r\mathcal{L}_1 + r^2\mathcal{L}_2 + \dots)u + \mathcal{N}_0(u, u) + r\mathcal{N}_1(u, u) + \dots \\ &= (\mathcal{L}_0 + (r_1\epsilon + r_2\epsilon^2 + \dots)\mathcal{L}_1 + (r_1\epsilon + r_2\epsilon^2 + \dots)^2\mathcal{L}_2 + \dots)(u_1\epsilon + u_2\epsilon^2 + \dots) \\ &\quad + \epsilon^2\mathcal{N}_0(u_1, u_1) + 2\epsilon^3\mathcal{N}_0(u_1, u_2) + \dots + (r_1\epsilon + r_2\epsilon^2 + \dots)\epsilon^2\mathcal{N}_1(u_1, u_1) + \dots \end{aligned} \quad (70)$$

Separating orders in  $\epsilon$  leads to

$$0 = \mathcal{L}_0 u_1 \quad (71)$$

$$0 = \mathcal{L}_0 u_2 + r_1 \mathcal{L}_1 u_1 + \mathcal{N}_0(u_1, u_1) \quad (72)$$

$$0 = \mathcal{L}_0 u_3 + r_1 \mathcal{L}_1 u_2 + r_2 \mathcal{L}_1 u_1 + r_1^2 \mathcal{L}_2 u_1 + 2\mathcal{N}_0(u_1, u_2) + r_1 \mathcal{N}_1(u_1, u_1) \quad (73)$$

Equation (71) states that  $u_1$  is proportional to the bifurcating null vector. Because we have not yet defined  $\epsilon$ , we may take

$$u_1 = \zeta \quad (74)$$

Equation (72) involves the singular operator  $\mathcal{L}_0$  to which we apply the Fredholm alternative. We take the inner product of  $\zeta^\dagger$  with (72):

$$0 = \langle \zeta^\dagger, \mathcal{L}_0 u_2 \rangle + r_1 \langle \zeta^\dagger, \mathcal{L}_1 \zeta \rangle + \langle \zeta^\dagger, \mathcal{N}_0(\zeta, \zeta) \rangle \quad (75)$$

We deduce that

$$r_1 = -\frac{\langle \zeta^\dagger, \mathcal{N}_0(\zeta, \zeta) \rangle}{\langle \zeta^\dagger, \mathcal{L}_1 \zeta \rangle} \quad (76)$$

We then write

$$\epsilon \approx \frac{r}{r_1} \quad (77)$$

$$u \approx \epsilon \zeta = \frac{r}{r_1} \zeta = -\frac{\langle \zeta^\dagger, \mathcal{L}_1 \zeta \rangle}{\langle \zeta^\dagger, \mathcal{N}_0(\zeta, \zeta) \rangle} r \zeta \quad (78)$$

Moreover, with  $r_1$  as in (76), we can solve (72) for  $u_2$ :

$$\mathcal{L}_0 u_2 = -r_1 \mathcal{L}_1 \zeta - \mathcal{N}_0(\zeta, \zeta) \quad (79)$$

Although (67) insures that the denominator in (76) is non-zero, it may happen that the numerator of (76) is zero. This is in fact what happens in the case of a pitchfork bifurcation. We must then continue to higher order to obtain a first approximation to the solution  $u$ . We simplify (73) using  $r_1 = 0$  and  $u_1 = \zeta$

$$0 = \mathcal{L}_0 u_3 + r_2 \mathcal{L}_1 u_1 + 2\mathcal{N}_0(u_1, u_2) \quad (80)$$

where  $u_2$  is known via (79). We now take the inner product with  $\zeta^\dagger$ :

$$0 = \langle \zeta^\dagger, \mathcal{L}_0 u_3 \rangle + r_2 \langle \zeta^\dagger, \mathcal{L}_1 \zeta \rangle + 2\langle \zeta^\dagger, \mathcal{N}_0(\zeta, u_2) \rangle \quad (81)$$

We deduce that

$$r_2 = \frac{-2\langle \zeta^\dagger, \mathcal{N}_0(\zeta, u_2) \rangle}{\langle \zeta^\dagger, \mathcal{L}_1 \zeta \rangle} \quad (82)$$

We then write

$$\epsilon^2 \approx \frac{r}{r_2} \quad (83)$$

$$u \approx \epsilon \zeta = \sqrt{\frac{r}{r_2}} \zeta \quad (84)$$

The expansion (78) corresponds to a transcritical bifurcation ( $u \sim r\zeta$ ) and the expansion (84) to a pitchfork bifurcation ( $u \sim \sqrt{r}\zeta$ ). Since we have written (63) such that  $u = 0$  is always a steady solution, saddle-node bifurcations, which do not involve the transverse intersection of branches, must be treated in a slightly different manner, which we will not do here.

## 4 Some other model dynamical systems

We have studied in detail the Lorenz model, the logistic map, the sine circle map, the Barkley model, the Swift-Hohenberg and real Ginzburg-Landau equations and the kicked rotor. Many other model dynamical systems have played a role in the recent explosion of the field, and which you may encounter, but which we did not get a chance to study. We present some of them briefly here.

### 4.1 Rössler system

The Rössler system

$$\dot{x} = -y - z \quad (85a)$$

$$\dot{y} = x + ay \quad (85b)$$

$$\dot{z} = b + z(x - c) \quad (85c)$$

was proposed in 1976 by Otto Rössler (University of Tübingen, Germany) There are two fixed points, both with a complex conjugate pair of eigenvalues and one real eigenvalue. For one fixed point the c.c. pair has positive real part and the real eigenvalue is negative (and vice versa for the other one). Trajectories spiral outwards (c.c. pair) from the first fixed point and eventually return to it (negative real eigenvalue). This system also undergoes a period-doubling cascade, when two of the parameters  $a$ ,  $b$ ,  $c$  are fixed and the third is varied.

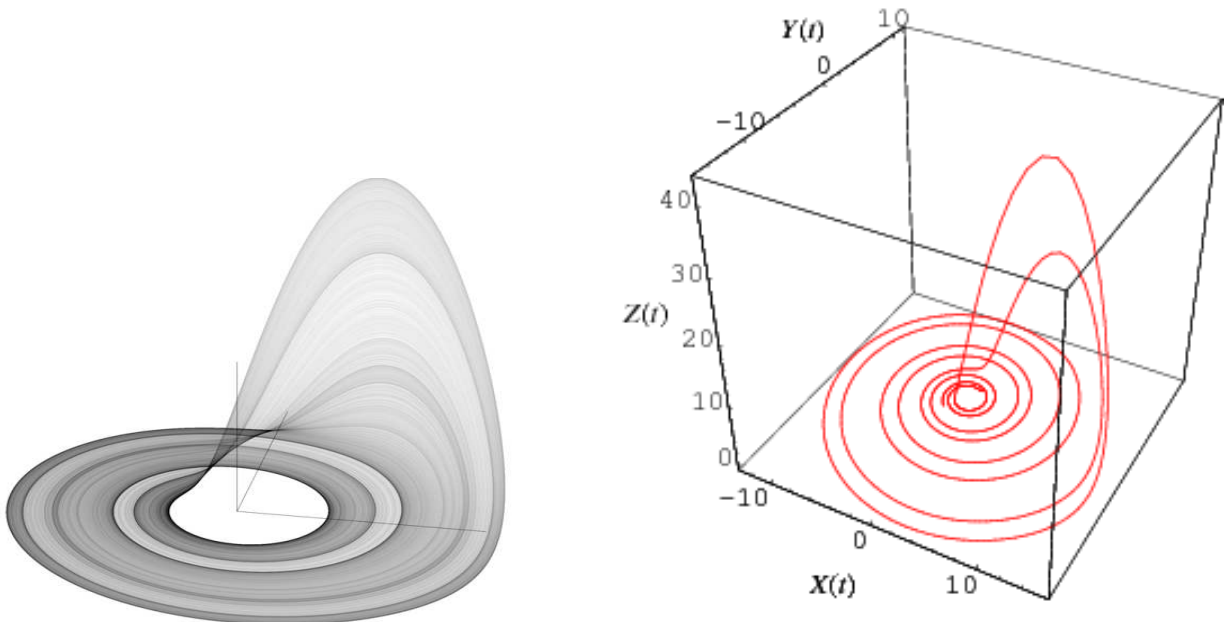


Figure 14: Rössler attractor. Left: from [http://en.wikipedia.org/wiki/Rossler\\_attractor](http://en.wikipedia.org/wiki/Rossler_attractor). Right: from <http://mathworld.wolfram.com/RoesslerAttractor.html>.

## 4.2 Van der Pol oscillator

$$\ddot{x} - \epsilon(1 - x^2)\dot{x} + x = F \cos(\omega_f t) \quad (86)$$

This is a harmonic oscillator to which nonlinear damping and forcing have been added. When the forcing is zero, (86) can be written as

$$\dot{x} = y \quad (87a)$$

$$\dot{y} = \epsilon(1 - x^2)y - x \quad (87b)$$

Scholarpedia has an extensive website on the van der Pol oscillator (with animations) by T. Kanamaru.

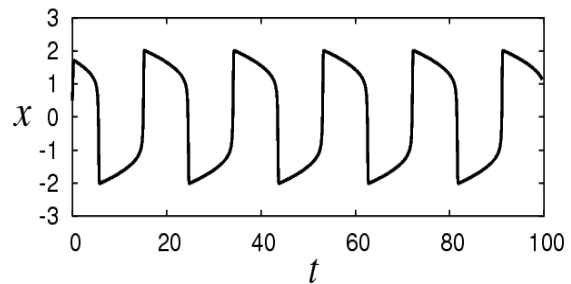
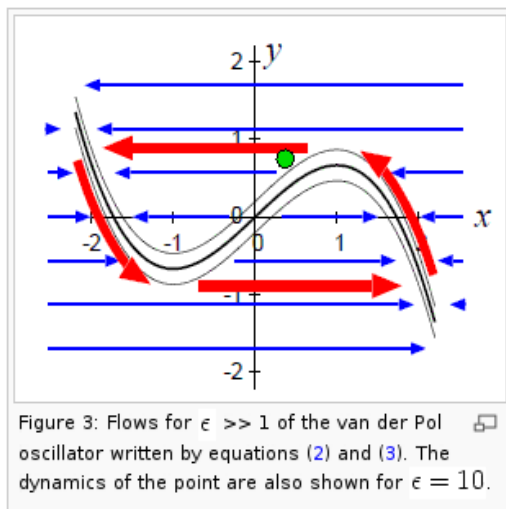


Figure 15: Van der Pol oscillator. Left: Nullclines in the  $(x, y) = (x, \dot{x})$  plane. Right: timeseries showing relaxation oscillations. From T. Kanamura, *Van der Pol oscillator*, Scholarpedia 2(1):2202

## 4.3 Duffing oscillator

The Duffing oscillator is governed by the equation

$$\ddot{x} + \delta\dot{x} - x + x^3 = \gamma \cos(\omega t) \quad (88)$$

In contrast to the van der Pol oscillator, here the damping ( $\delta\dot{x}$ ) is linear, but there is a nonlinear potential  $V(x^4/4 - x^2/2)$ .

Scholarpedia has an extensive website (with animations) on the Duffing oscillator by T. Kanamaru.

## 4.4 Hénon map

$$x_{n+1} = y_n + 1 - ax_n^2 \quad (89a)$$

$$y_{n+1} = bx_n \quad (89b)$$

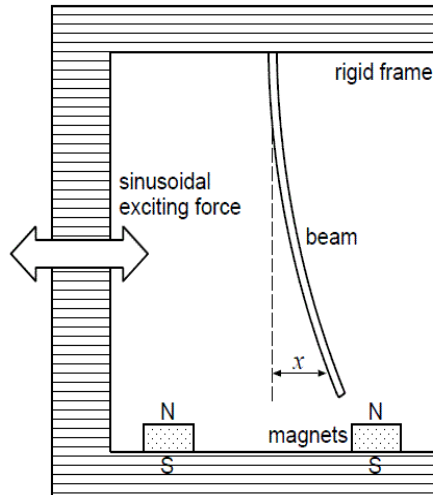


Figure 16: The Duffing oscillator describes the behavior of the magneto-elastic beam.

The Hénon map was introduced by Michel Hénon (Observatoire de Nice, France) in 1976. The website <http://ibiblio.org/e-notes/Chaos/henon.htm> by Evgeny Demidov has an extensive treatment of the Hénon map. Its actions of **stretching and folding** are an essential part of chaos and are shared by other prototypical maps, such as the **Smale Horseshoe** and the **Baker's Map**. See figure 17.

#### 4.5 Reaction-Diffusion Systems

We already mentioned the FitzHugh-Nagumo equations and the Barkley model. Here are two more reaction-diffusion systems.

The **Brusselator**:

$$f(u, v) = a + u^2v - bu - u \quad (90a)$$

$$g(u, v) = bu - u^2v \quad (90b)$$

was formulated by the group of I. Prigogine in Belgium to describe autocatalytic reactions. Prigogine was interested in irreversibility in quantum mechanics and was one of the pioneers of the study of oscillating chemical reactions. He was awarded the Nobel Prize in Chemistry in 1977.

The **Gray-Scott model**:

$$f(u, v) = -uv^2 + a(1 - u) \quad (91a)$$

$$g(u, v) = uv^2 - (1 + k)v \quad (91b)$$

forms self-replicating spots, as seen in figure 18.

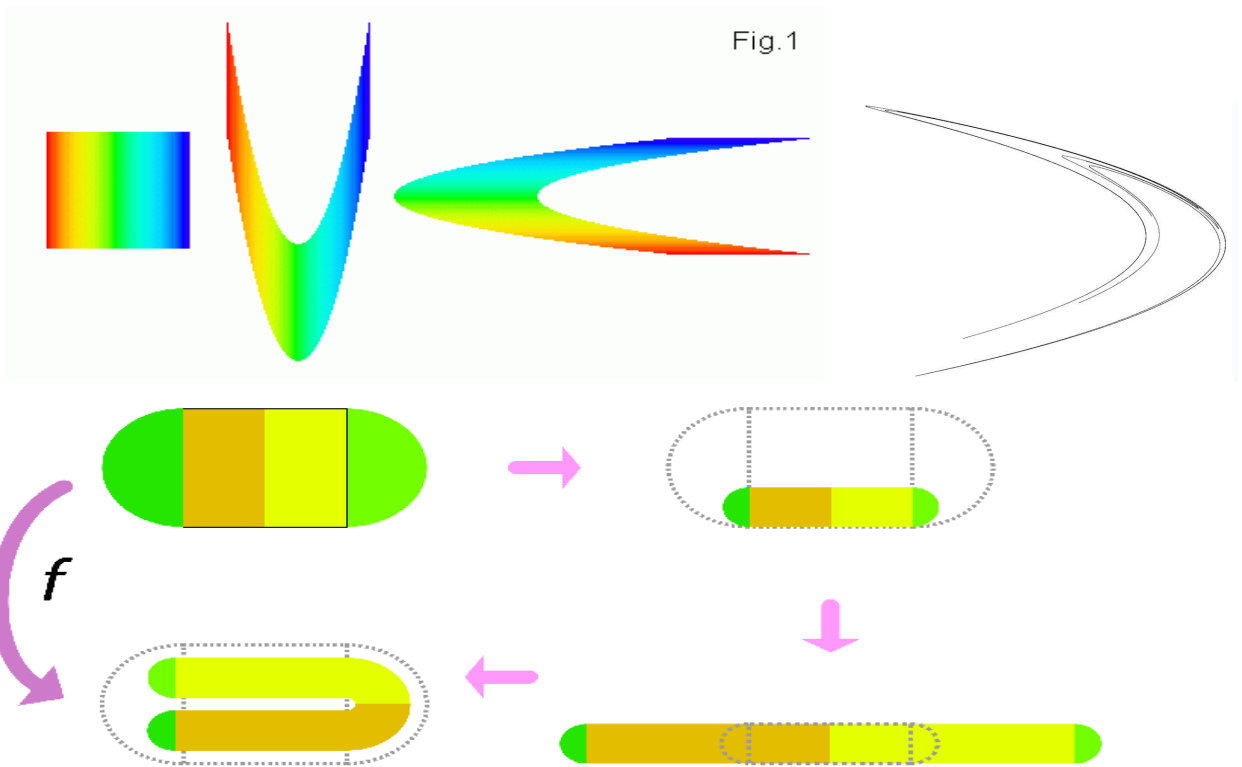


Figure 17: Above: Hénon map. Left: Hénon map explained as a decomposition of three operations: stretching, folding, and rotation. From E. Demidov, <http://ibiblio.org/e-notes/Chaos/henon.htm>. Right: Attractor of Hénon map for  $a = 1.4$  and  $b = 0.3$ . From [http://en.wikipedia.org/wiki/Henon\\_map](http://en.wikipedia.org/wiki/Henon_map). Below: Smale horseshoe map composes stretching and folding. From <http://commons.wikimedia.org/wiki/>

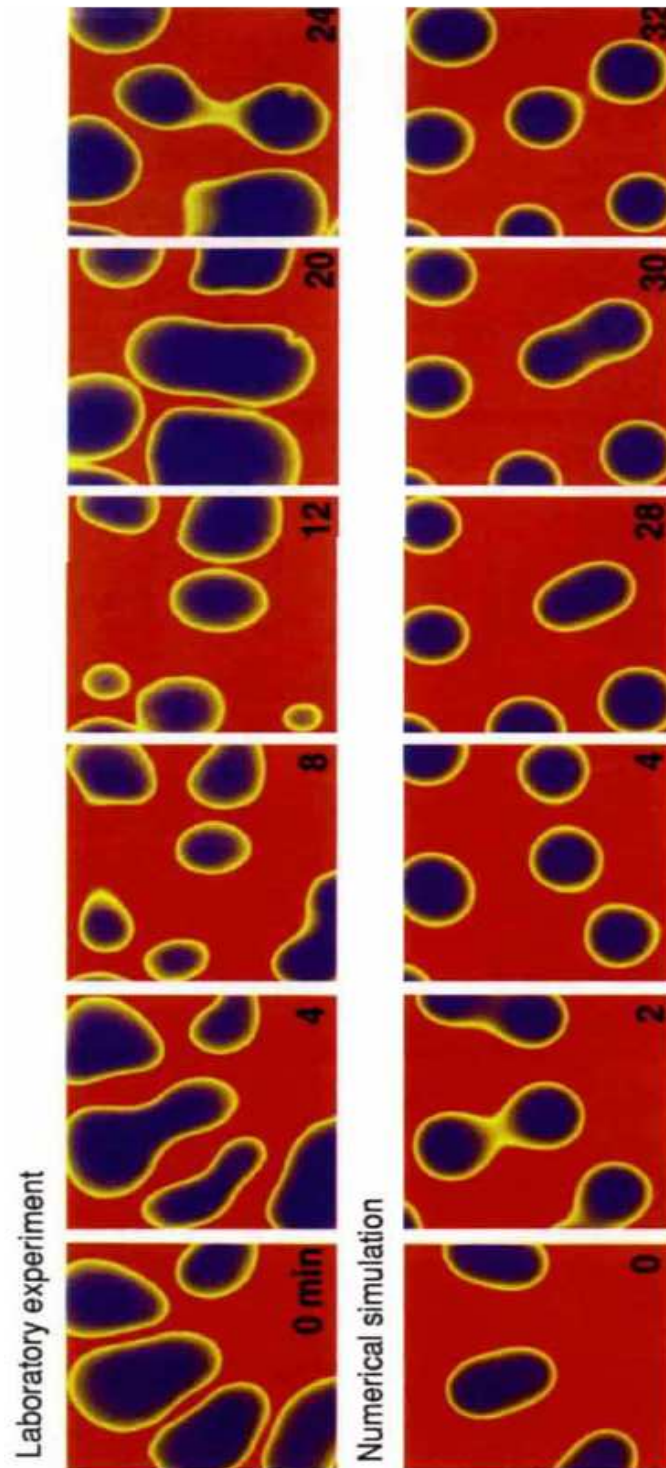


Figure 18: Laboratory chemical experiment compared with simulations of the Grey-Scott model. From K. Lee, W.D. McCormick, J.E. Pearson & H.L. Swinney, *Experimental observation of self-replicating spots in a reaction-diffusion system*, Nature **369**, 215 (1994).

## 4.6 Burgers' equation

**Burgers' equation:**

$$u_t + uu_x = \nu u_{xx} \quad (92)$$

was formulated by J.M. Burgers and has a clear correspondence to hydrodynamics. If  $\nu = 0$ , then shocks can appear and the equation is used to model gas dynamics and traffic flow. If  $\nu \neq 0$ , the Cole-Hopf transformation

$$u = -2\nu\phi_x/\phi \quad (93)$$

transforms (92) into the diffusion equation.

$$\phi_t = \nu\phi_{xx} \quad (94)$$

## 4.7 Kuramoto-Sivashinsky equation

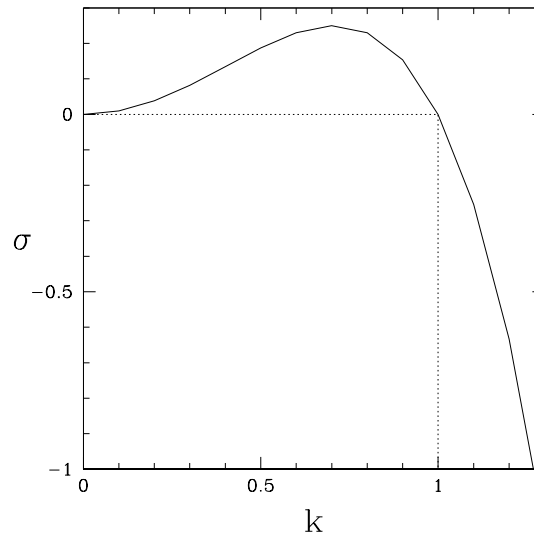


Figure 19: Growth rate  $\sigma$  as a function of spatial wavenumber  $k$  for the Kuramoto-Sivashinsky equation. The trivial  $u = 0$  state is unstable to periodic perturbations with wavenumbers  $0 < k < 1$ .

The **Kuramoto-Sivashinsky equation:**

$$u_t + uu_x = -u_{xx} - u_{xxxx} \quad x \in [-L/2, L/2] \quad (95)$$

also has a clear correspondence to hydrodynamics. However, the second derivative term  $-u_{xx}$  has a negative sign and so is destabilizing instead of stabilizing: substituting  $u \sim \sin kx$  leads to  $+k^2u$  on the right-hand side. In the K-S equation, it is the fourth derivative term  $-u_{xxxx}$  which is stabilizing: substituting  $u \sim \sin kx$  leads to  $-k^4u$  on the right-hand side. Boundary conditions can be periodic, or Dirichlet or Neumann (four Dirichlet or Neumann conditions are needed for this fourth-order equation). The K-S equation was originally formulated to describe flame fronts.

For periodic boundary conditions, linear instability of the trivial  $u = 0$  solution to  $\sin kx$  is governed by

$$\sigma = k^2 - k^4 \tag{96}$$

shown in figure 19, where it can be seen that the unstable wavenumbers are  $0 < k < 1$ . Allowed values of the wavenumber  $k$ , i.e. those which can fit into the box of length  $L$ , are multiples of  $2\pi/L$ . If  $L < 2\pi$ , then  $k_{\min} = 2\pi/L > 1$  and so  $u = 0$  is stable. As the size  $L$  of the box is increased, an increasing number of unstable wavenumbers can fit, leading to more bifurcations from the trivial state. There exists a large number of solutions to the Kuramoto-Sivashinsky equation, even for fixed  $L$ . Some solutions are shown in figure 20.

#### **4.8 Cross-Newell equations**

Cross and Newell have considered the spatial phase  $\theta(X, Y, T)$  and its gradient  $\mathbf{k} = \nabla\theta$  of a system of convection rolls or a more general striped pattern and formulated evolution equations for these fields.

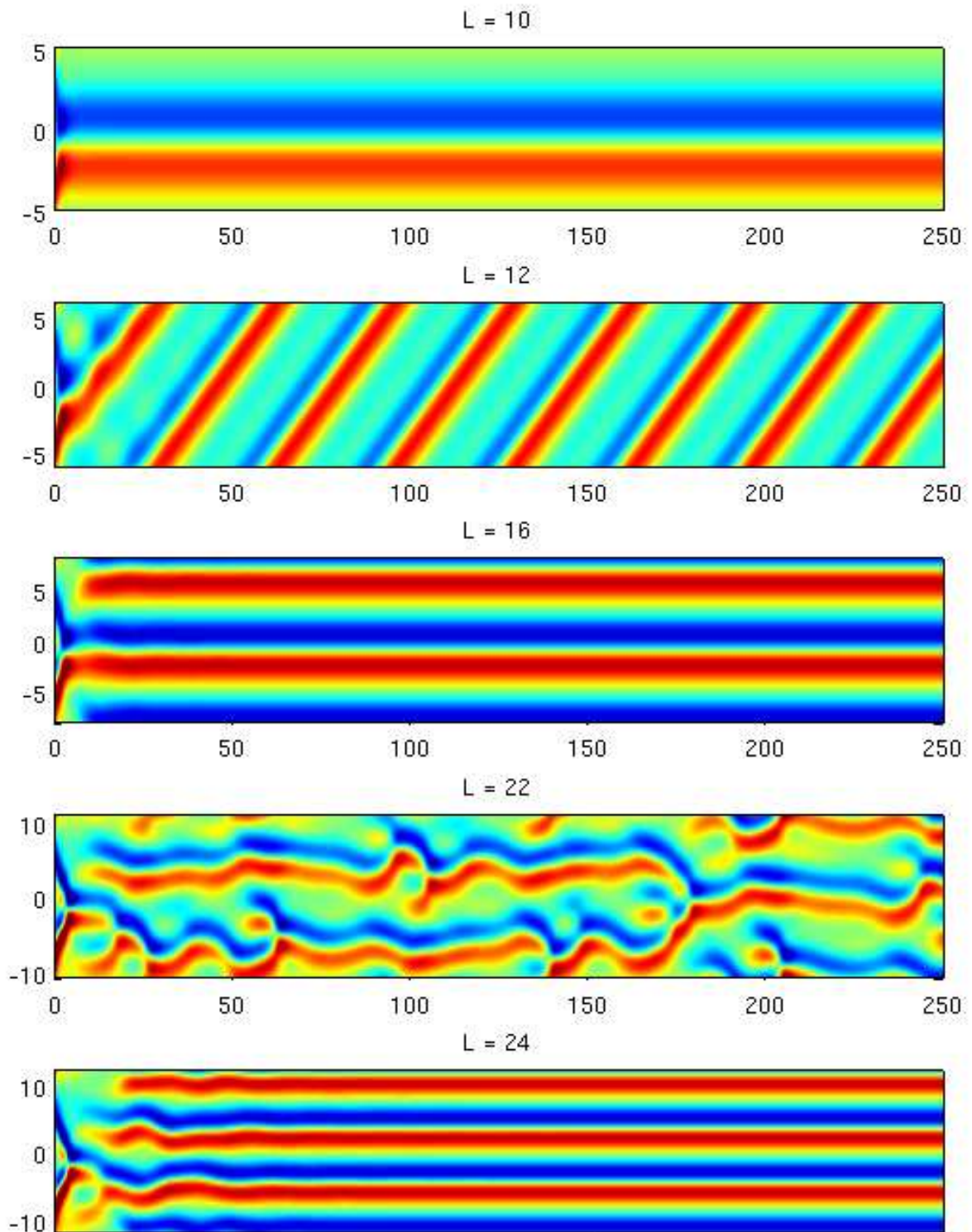


Figure 20: Some solutions to the Kuramoto-Sivashinsky equation for lengths  $L = 10, 12, 16, 22, 24$ . Horizontal axis is  $t$ , vertical axis is  $x$ . From P. Cvitanović et al., <http://chaosbook.org>